

# **Journal of Mechanical Engineering and Research Developments**

**Volume - 13**

**Issue- 2**

**May - August 2025**



**ENRICHED PUBLICATIONS PVT.LTD**

**JE - 18,Gupta Colony, Khirki Extn,  
Malviya Nagar, New Delhi - 110017.**

**E- Mail: [info@enrichedpublication.com](mailto:info@enrichedpublication.com)**

**Phone :- +91-8877340707**

# Journal of Mechanical Engineering and Research Developments

## **Aims and Scope**

Subject areas include, but are not limited to the following fields:

- Aerodynamics
- Aerothermodynamics
- Automotive Engineering
- Computer Aided Engineering
- Component Manufacturing
- Conveyors
- Energy Studies
- Engines and Turbines
- Engineering Education

# Journal of Mechanical Engineering and Research Developments

**Managing Editor**  
**Mr. Amit Prasad**

## **Editorial Board Member**

**Dr. Gurbhinder Singh Brar**

Professor and Head  
Deputy Dean Research  
Guru Kashi University,  
Talwandi Sabo  
gurbhinder@yahoo.com

**V K Jadon**

Dean of Baddi University of Emerging  
Sciences and Technology, Baddi  
vkjadon@yahoo.com

**Dr. Velagapudi Vasu**

Asst. Professor,  
NIT, Warangal  
vvvasu@rediffmail.com



# Journal of Mechanical Engineering Research and Developments

(Volume No. 13, Issue No. 2, May - August 2025)

## Contents

Sr. No.	Articles Name / Authors	Page No
1	Withdrawal Behaviour Through a Single Round Hole In a Cross Flow - <i>A. K. M. Sadrul Islam' .I. J. McGuirk''</i>	1 - 12
2	Autoignition of Natural Gas Fuelled Engines -A Review of its Possibilities - <i>Sii How Sing Masjuki Hassan Mohd. Zaki Abdulmuin</i>	13 - 20
3	Computation Studies of Aii Flow/ in Two Dimensional Coaxial Pipe - <i>Adi Surjosatyo and Farid Nasir Ani Ji-Huan He</i>	21 - 32
4	A Classical Generalized Variational Principle for Pseudo-StateThermoelasticity of Piezoelectric Materials - <i>Ji-Huan He</i>	33 - 36

▪



# Withdrawal Behaviour Through a Single Round Hole In a Cross Flow

A. K. M. Sadrul Islam' .I. J. McGuirk''

## ABSTRACT

Experimental measurements of drawdown, the critical withdrawal rate and the mean temperature profiles in the near field region of a withdrawal system in a two-layered thermally stratified cross-flow are presented. Flow visualisation is also reported which provides detail information on the structure and dynamics of the warm/cold water interfaces for different intake flow rates. The present experimental data on the critical intake flow rate are compared with the measurements of Goldring (1984). The drawdown results indicate an inverse dependency on density gradient unlike the case without cross flow.

## NOMENCLATURE

$D$	hydraulic diameter, $4 \times \text{area} / \text{wetted perimeter}$	$h_2$	depth of cold water layer
$DD$	drawdown fraction, $(T_o - T_2) / (T_1 - T_2)$	$H$	$h_1 + h_2$
$DD_m$	peak drawdown fraction	$Q_o$	intake flow rate
$Fr_o$	Inlet Froude number, $U / (g'H)^{1/2}$	$Q_o^c$	critical intake flow rate
$g$	gravitational acceleration	$U$	cross flow velocity
$g'$	reduced gravitational acceleration, $g \Delta\rho / \rho_1$	$Re$	Reynolds number, $UD/\nu$
$h_1$	depth of warm water layer	$T$	mean temperature of the field
$X, Y, Z$	cartesian coordinates measured from the axis of the intake hole	$T_1$	temperature of warm water
$\Phi$	normalised temperature, $(T - T_2) / (T_1 - T_2)$	$T_2$	temperature of cold water
$\rho_1$	density of warm water	$T_o$	mean temperature of the intake flow
$\rho_2$	density of cold water		
$\Delta\rho$	density difference, $(\rho_2 - \rho_1)$		
$\nu$	kinematic viscosity		

## INTRODUCTION

In natural water bodies density stratification is caused by the presence of a varying temperature with depth due to variation of observed solar radiation, also by a vertical profile in the concentration of

dissolved and suspended solids. This naturally occurring stratification is sometimes enhanced by the rejection of large volumes of waste heat from coastal power stations in the form of a warm water discharge which tends to form a low density floating surface layer. This type of stratification is usually of stable nature and is important in several flow problems of engineering interest, e.g. management systems for water quality control in reservoirs, waste or warm water discharges into natural water bodies and cooling water intake from reservoirs, seas and rivers. In many of these flows the density variation combines with gravity to produce buoyancy effects which can crucially influence the fluid dynamic behaviour. The buoyancy force inhibits vertical motion and in some engineering problem, specially the management of water quality of reservoirs and the intake of cooling water, the flow is coming from a spatially limited selective layer or region. This phenomena is known as selective withdrawal. Selective withdrawal phenomenon has often been studied for two dimensional laminar flow cases. Brooks and Koh (1969) and Imberger (1980) have provided a very good review of these cases. In practice, specially for the intake of cooling water, this phenomena is of three dimensional (3D) nature, and needs an extensive study. This paper deals with this type of 3D problem. A single round hole is considered for the intake geometry to withdraw selectively cold water from a two layered thermally stratified cross flow.

## EXPERIMENTAL SETUP AND PROCEDURE

The experiments were carried out in a flume of 0.4m width, 0.5m depth and 6m length. The withdrawal hole was situated on the smooth wooden bottom surface at the symmetry axis of the flume, 2.5m downstream of the entry section. The warm and cold water were introduced into the flume from two constant head tanks and the heights of the warm and cold water layers were maintained by means of a splitter plate. Figure 1 shows a schematic view of the experimental flume.

Goldring (1984) obtained experimental correlations for critical drawdown conditions for different cross-flow and intake hole diameter conditions. In the present study, Goldring's experiment was extended with single round hole to study the mixing behaviour in the near field region of the intake system. The diameter of the hole was  $d=42.5$  mm and the cross-flow velocity was  $U=31.25$  mm/sec for both layers. Seven experimental runs were made to map the temperature field at two Reynolds numbers, 8330 and 9850 and the inlet Froude number,  $Fr$ , ranges from 0.72 to 1.3. Table 1 gives the details of the parameters of these seven experimental runs.

The water temperature was measured by means of nine miniature bead (1.5 mm dia) thermistors (S Data ISL-142) calibrated to an accuracy of  $\pm 0.01^\circ\text{C}$ ; six

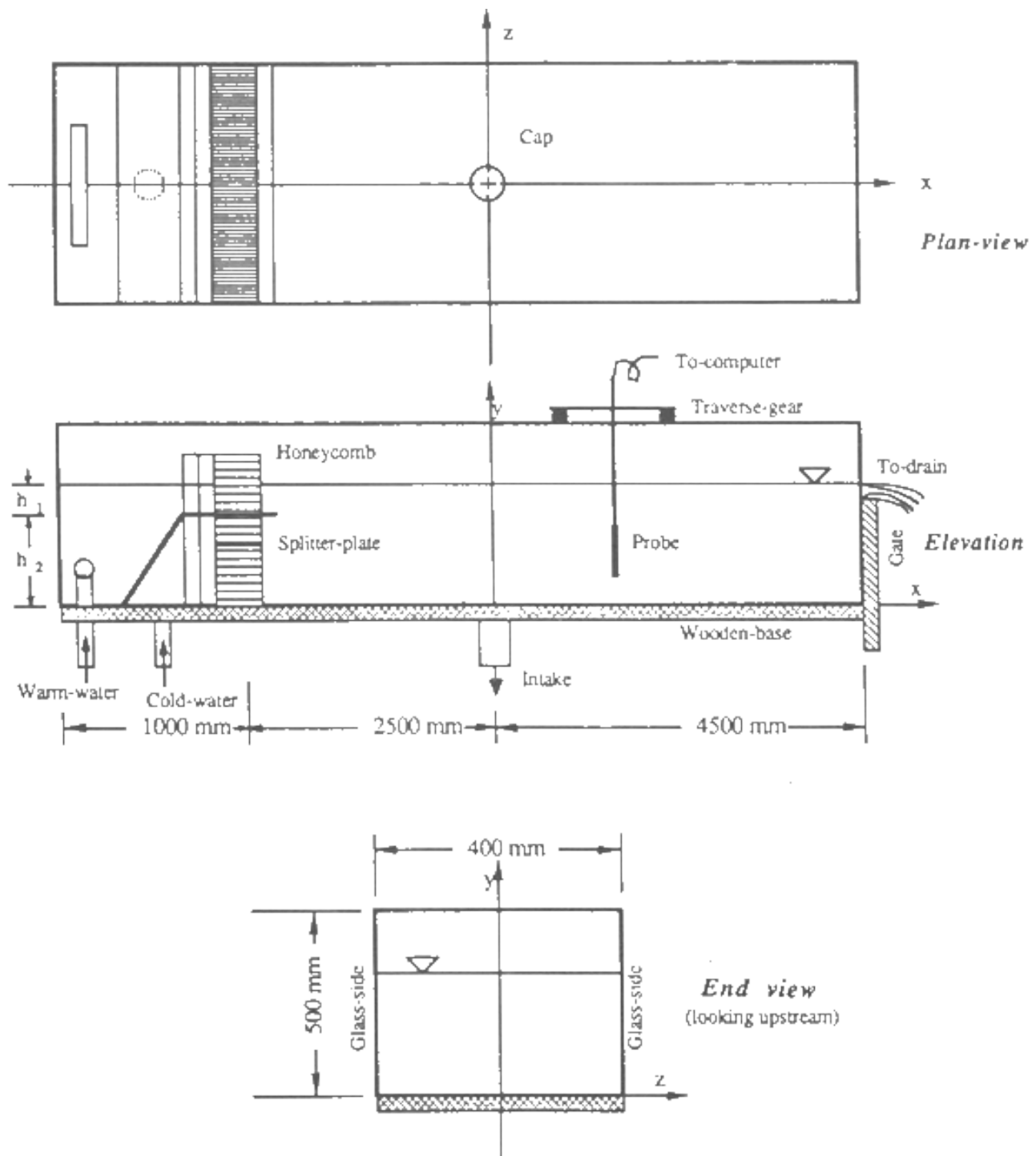


Fig. 1 The cross-flow flume.

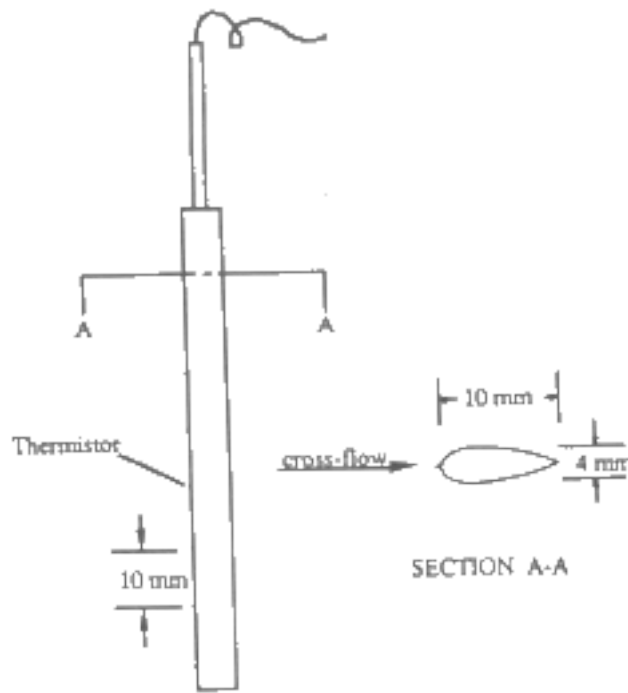


Fig. 2 (a) The probe for field temperature measurements.

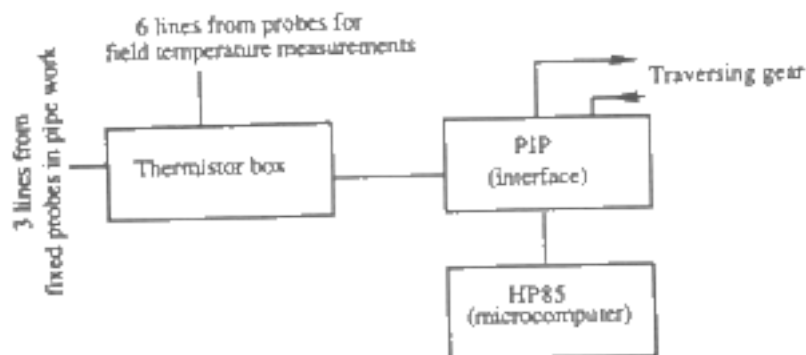


Fig. 2 (b) Block diagram for electrical connection of thermistor probes and traversing gear to the microcomputer.

of which was for field temperature mapping. The thermistor box which converts the millivolt (mv) signal to an equivalent resistance and then an analogue signal which was digitised by an interface (Plant Interface Peripheral) and sent to a Hewlett Packard HP85 microcomputer where an equivalent temperature reading ( $^{\circ}\text{C}$ ) was recorded. Fig. 2(b) illustrates these connections by a block diagram. The field temperature thermistors were fixed on a small (10mm x 5mm) stream lined plastic rod, (fig. 2a) which was traversed by a traversing gear monitored by the microcomputer. The time taken by the system for sampling readings for the nine thermistors and converting the readings into temperature ( $^{\circ}\text{C}$ )

was approximately 1 second.

The temperature field in the wake of the hole was observed to fluctuate due to the turbulence created by the flow disturbance caused by the intake system. The amplitude of these fluctuations increased with the intake flow rate. To average out these fluctuations, different sample sizes ranging from 30 to 300 depending upon the flow condition were taken.

## FLOW VISUALISATION

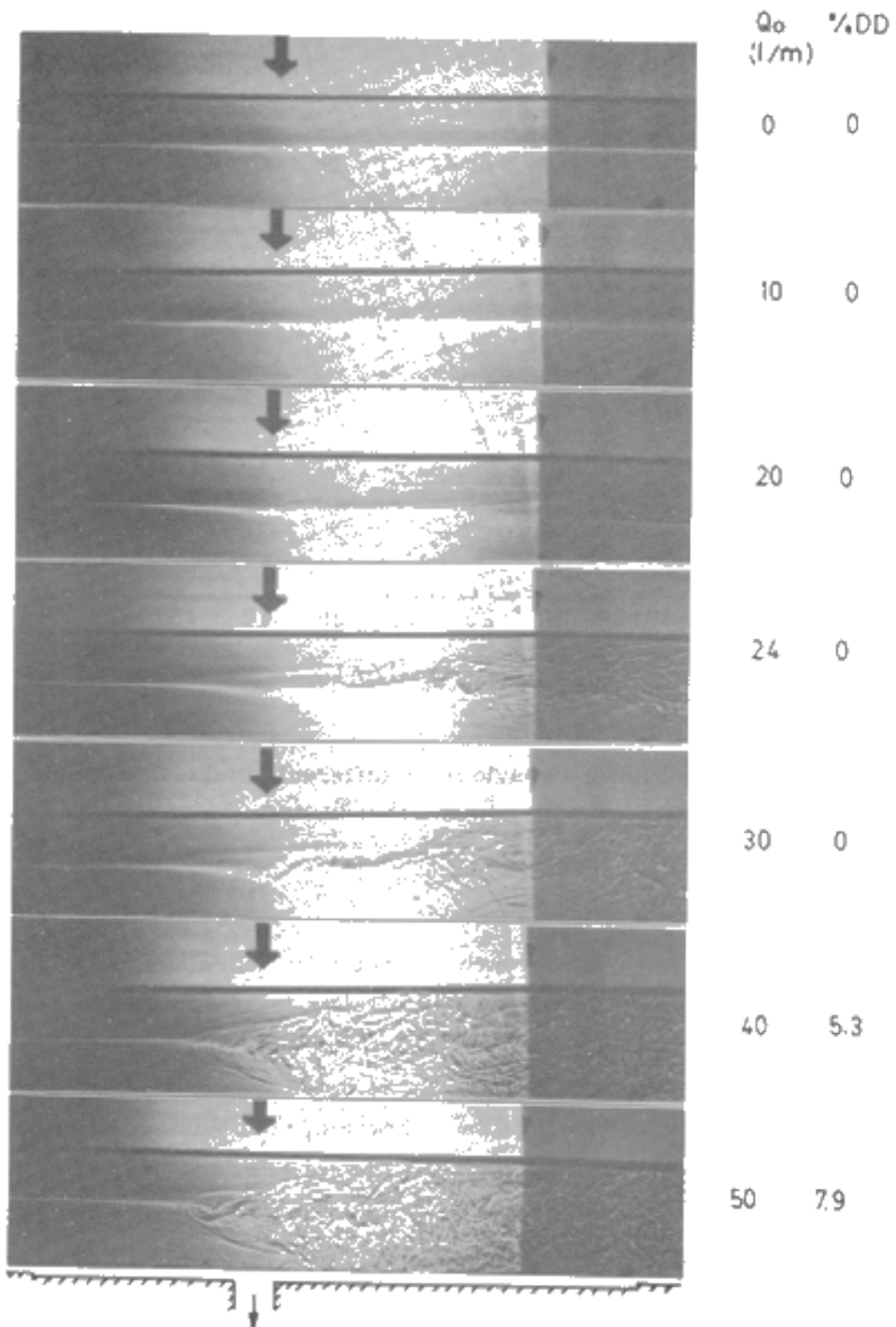
Shadowgraph technique was used to capture the features of the mixing and disturbance created in the wake of the intake system (hole). Figure 3 shows photographs taken from shadowgraph images for no intake flow rate and six different intake flow rates before and after the incipient (critical) drawdown occurs. It can be seen from the photographs that upstream of the hole the buoyancy has damped out all entrainment, the interface thickness remains constant and the flow becomes laminar and two dimensional. As the intake flow rate increases the turbulence generated at the hole breaks up the interface and in the wake region the two layers are mixed up and the mixed layer is pulled down towards the hole, causing a significant proportion of drawdown.

## EXPERIMENTAL RESULTS AND DISCUSSION

The drawdown fraction (DD) is calculated with the mean temperature of the intake flow. Since the temperature of the intake flow fluctuates and this fluctuation also depends on the intake flow rate, the mean temperature was obtained by averaging 100-600 samples depending on the intake flow condition. Figure 4 shows a typical drawdown behaviour at different intake flow rates. After drawdown onset the drawdown fraction increases linearly with  $Q$  and then tends towards an asymptotic value. The critical intake flow rate,  $Q_0$  was obtained by the projection of the linear portion of the drawdown curve to the  $DD = 0$  line (after the practice of Jirka & Katavola, 1979 and Goldring 1984). The asymptotic (or peak) value observed in the drawdown curve has a great practical importance in the context of intake system design. For example, for the case of fig. 4, for well mixed conditions at the upstream the drawdown will be

$$DD_m = \frac{h_1}{h_1 + h_2} = 20\%$$

which gives a defining limit for selective withdrawal (see appendix for derivation). For  $DD > DD^*$ , the intake system selectively withdraws water from warm upper layer and for  $DD < DD^*$  it withdraws selectively from the cold lower layer. The optimum system is therefore that which leads to a maximum reduction in the peak drawdown value below  $DD^*$ . During the present experimental studies, the peak DD observed were always substantially below  $DD^*$ .



Shadowgraph pictures for plain hole intake system  
at different intake flow rates.  $h_1 = 50$  mm,  $h_2 = 80$  mm,  
 $T_1 = 9.4^\circ\text{C}$ ,  $T_2 = 4.6^\circ\text{C}$

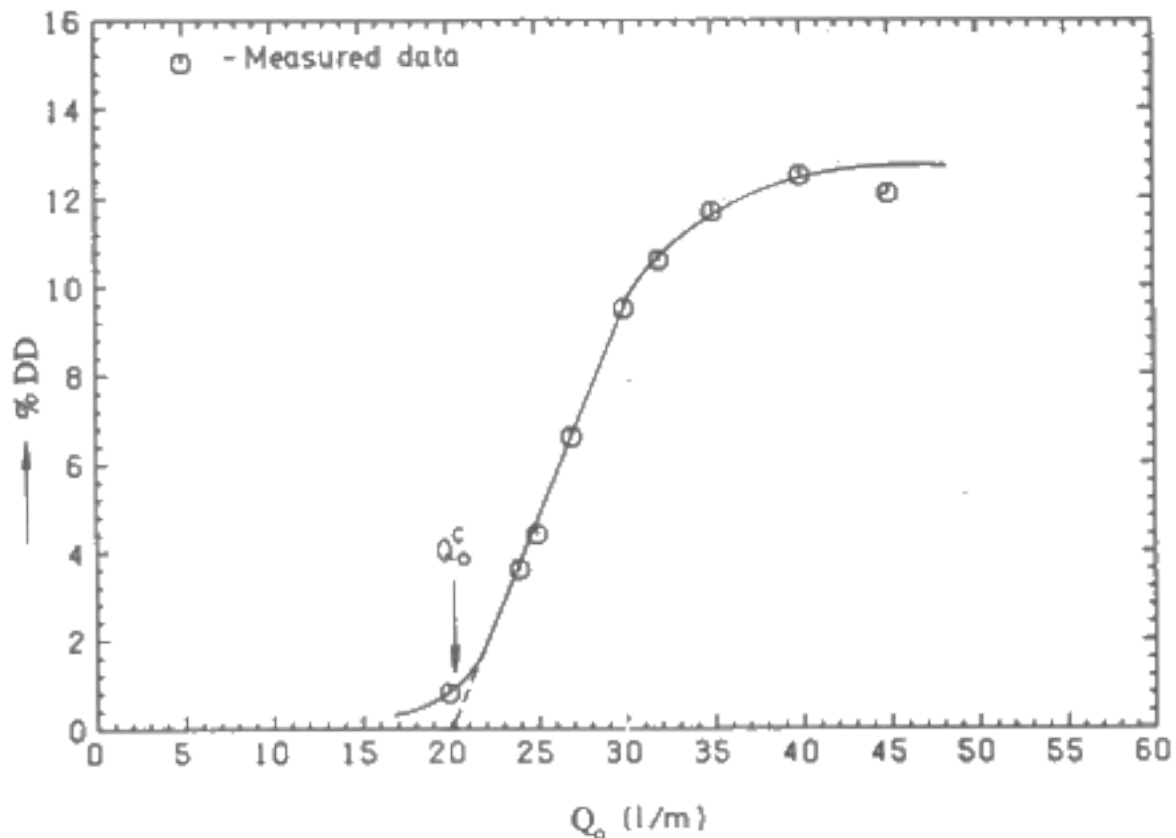


Fig. 4 : Drawdown behaviour at different intake flow rates for  $h_1 = 20$  mm,  $h_2 = 80$  mm,  $\Delta T = 12^\circ\text{C}$ ,  $Fr_o = 0.72$  and  $Re = 8330$ .

showing that in all cases the intake system selectively withdrew water from the cold lower layer. Goldring (1984) did however report a few cases where the maximum DD values were slightly greater than DD-. The critical drawdown results of the present investigation are compared with the correlation equation (Goldring 1984) in fig. 5. The present measurements agree quite well with the correlation equation (1).

$$\frac{h_2}{d} \left( \frac{U}{\sqrt{g'h_2}} \right)^{0.575} = 0.763 \left( \frac{Q_o^c}{\sqrt{g'd^5}} \right)^{0.386} \quad (1)$$

Equation (1) reveals that for the cross-flow cases the critical intake flow rates,  $Q_o^c$  shows an inverse proportionality with density difference  $\Delta\rho$ , which is in direct contrast to the belief that the buoyancy inhibits drawdown, although this belief is supported by the axisymmetric withdrawal from stagnant environment. (see, Craya 1949, Harleman et al 1959, Goldring 1981, Ivey & Blake 1985, McGuirk & Islam 1987).

The effect of  $\Delta\rho$  on drawdown at different supercritical intake flow rates ( $Q_o > Q_o^c$ ) are also presented in

figure 6. By increasing  $Dr$ , the drawdown is increased.

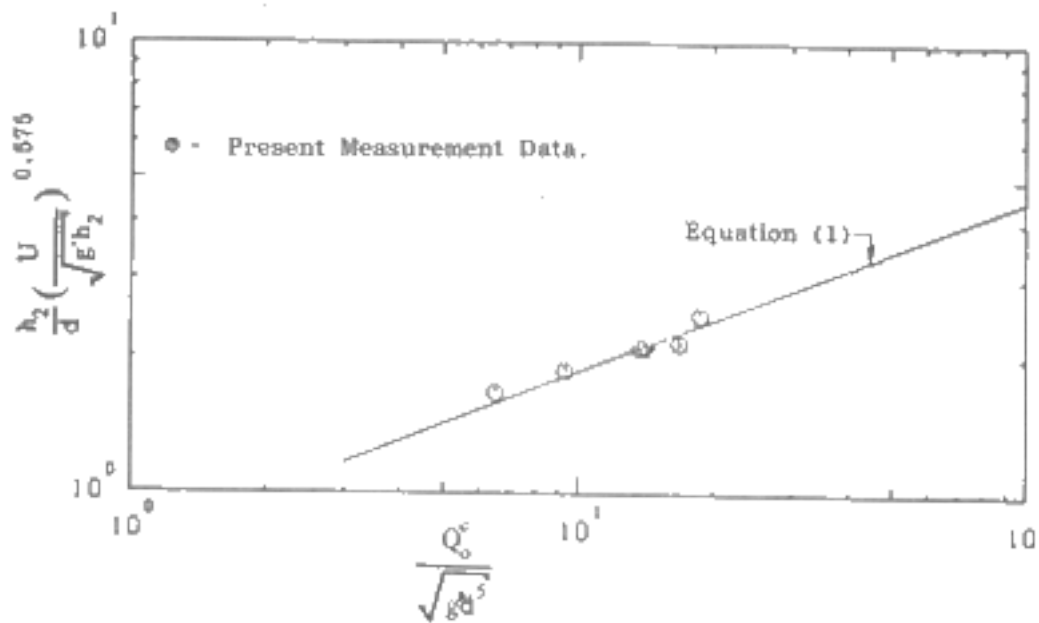


Fig. 5 : Critical drawdown.

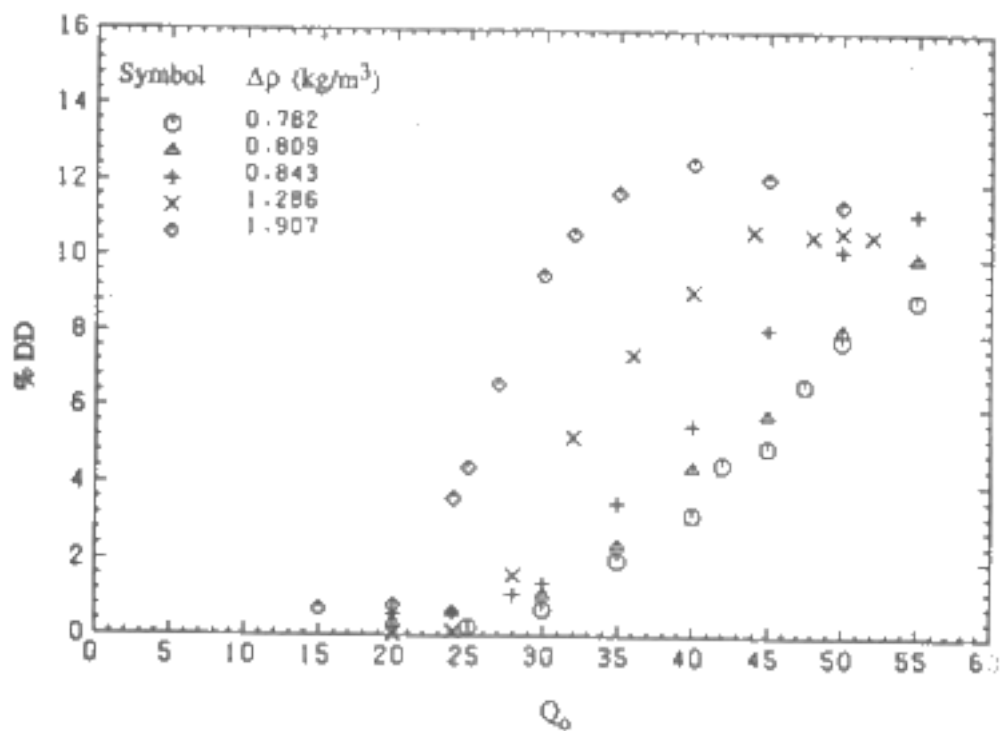
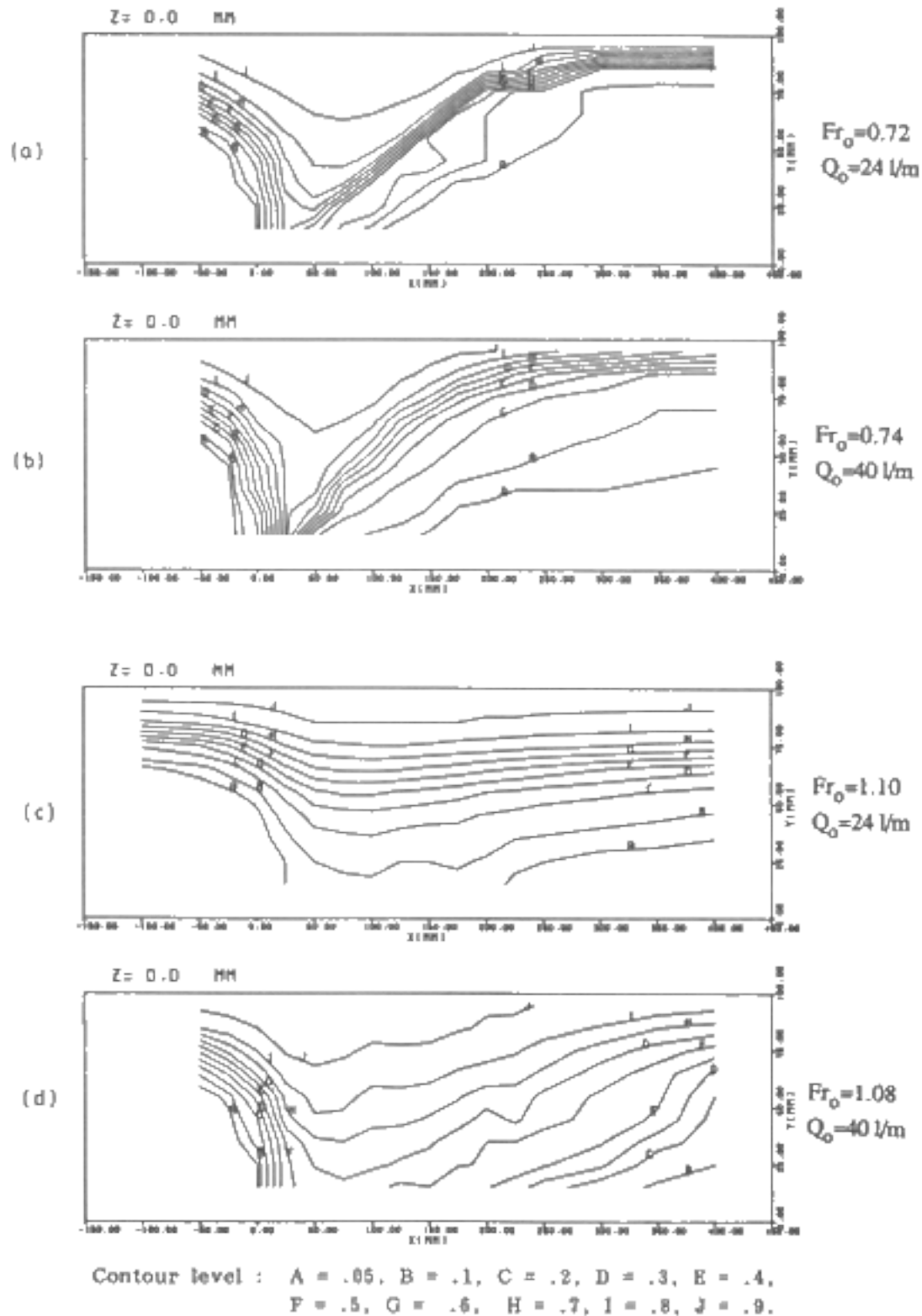


Fig. 6 Effect of buoyancy on drawdown,  $h_1=20\text{mm}$ ,  $h_2=80\text{mm}$



**Fig. 7 :** Measured contours of normalised temperature,  $\Phi$  on the symmetry plane.

The peak value of DD observed also increases with  $Dr$ . An explanation was given by Islam (1998) for these facts by observing the predicted flow and temperature field for these cases. The buoyancy forces,

proportional to the density gradient at the thermocline inhibit vertical motion of the fluid. For higher density gradient, this inhibiting process is stronger, so that less fluid is withdrawn vertically as the layer passes over the hole, and a larger fraction is drawn hence mixing the density differences are smaller. This mixed fluid leads then to higher drawdown fraction. This explanation is also supported by the measured temperature field shown in figure 7. Figure 7 shows the normalised temperature,  $F$  field on the symmetry plane. The measured perturbation of the temperature field in the near region of the hole is presented for approximately five different inlet Froude numbers and for two different intake flow rates. As  $Q$  increases, the vertical perturbation of a given temperature contour increases for the same Froude cases and causes more drawdown. For the same cases, the warm water floats up more quickly for the strong buoyant cases (less  $Fr$ ), but in the vicinity of the hole more warm waters are pulled down and causes more drawdown, which supports the explanation made above.

## CONCLUSIONS

The major conclusions from the present experimental observations may be summarised as follows :

- (i) Flow visualisation served as a good guide to understand the flow behaviour in the near field region of an intake system.
- (ii) The present drawdown data are in good agreement with the correlation equation (1) of Goldring, (1964) experimental data.
- (iii) An inverse dependency of density difference on  $Fr$  from the downstream, where due to more turbulence and critical intake flow rate,  $Fr_c$ , drawdown behaviour and peak DD value was observed, unlike the case without cross flow.

## ACKNOWLEDGEMENT

The work reported here was performed at Central Electricity Research lab, Leatherhead, U.K. and at Imperial College, London, U.K., during the tenure by the first author (A K N, I S I) with a British Commonwealth Scholarship.

## REFERENCES

1. Brooks N. H. & Koh. R. C. y. (1969) *Selective Withdrawal from Density Stratified Reservoirs*, J. Hydr. Divn, ASCE Vol.95, Hy4, pp.1366-1400.
2. Craya A. (1949) *Recherches Theoriques Sur L'Ecoulement de Coueches Superposees de Fluides de Densites Differentes*, "La Houille Blanche", pp.44-55.
3. Goldring B. T. (1964) *The effect of a hood on drawdown Criteria in Zero Crossflow*, Report No

RD/L/2031Ai81, Central Electricity Research Lab., Leatherhead, U.K.

4. Goldring B. T. (1984) .. *Setecrive Wirhrtrawal by Capped and uncapped inrakes in a Tidal flow,, Re\_porr'No TPRDn/267glNs+, cenrrar Ercctriciry Research Lab., Leatherhead, U. K.*

5. Flarlenran D. R. F., Morgan R. L. & purple R. A

6. Imberger, J. (1980) "*selective Withdrawal : A Review*", 2nd Int. Symp. on Stratified Flovs, IAHR, Norway, pp. 381-4

7. Ivey G. N. & Blake S. (1985) "*Axisymmetric Withdrawal and Inflow in a Density Stratified Container*", . J. Fluid Mech., Vol. 161, pp. 115-1

8. JirkaG. H. & KatavolaD. S. (1979) "*Supercritical*

9. McGuirk J. J. & Islam A. K. M. Sadrul (1987) "*Numerical Modelling of the Influence of a Hood onAxisymmetric Withdrawal from a Density Stratified Environment*", Proc.3rd Int. Symp. on Stratified Flows, Caltech, Pasadena, U.S.A.

i0.

Islam A.K.M. Sadrul (1988) "*Prediction of Selective Withdrawal Phenomenon in Stratified Cross Flowing Streams*", Ph.D. Thesis, Imperial JirkaG. H. & KatavolaD. S. (1979) "*Supercritical College, London, U.K.*

Table 1

Experimental Parameters for Intake Flow Through a Single Plain Hole:

Run No	$h_1$	$h_2$	$T_1$ °C	$T_2$ °C	$Q_o$ l/m	$Fr_o$	Re
1	50	80	12.4	7.6	24	1.28	9850
2	50	80	12.1	7.3	30	1.3	9850
3	50	80	12.3	7.6	40	1.29	9850
4	20	80	22.0	9.7	24	0.72	8330
5	20	80	21.3	9.3	40	0.74	8330
6	20	80	16.2	9.8	24	1.1	8330
7	20	80	16.3	9.7	40	1.08	8330

## Appendix

Drawdown fraction is defined as the ratio of the amount of the warm upper layer withdrawn to that of the total mixed fluid withdrawn and is expressed as :-

$$DD = \frac{m_{o,1}}{m_o} = \frac{m_{o,1}}{m_{o,1} + m_{o,2}} \quad \dots \dots \quad (A.1)$$

where  $m_o$  is the mass of the fluid withdrawn and the subscripts 1 and 2 refer to the masses of fluid withdrawn from the warm upper layer and cold lower layer respectively.

Now from mass balance,

$$m_o = m_{o,1} + m_{o,2} \quad (A.2)$$

and from energy balance,

$$m_o T_o = m_{o,1} T_1 + m_{o,2} T_2 \quad (\text{A.3})$$

assuming  $C_p$  of the fluid is constant in the range of temperature considered here,

Equating equations (A.2) and (A.3) we have,

$$DD = \frac{T_o - T_2}{T_1 - T_2}$$

For well mixed conditions at the upstream of the intake hole, the intake mass flow rate will be,

$$m_o = k(m_1 + m_2) \quad (\text{A.4})$$

where  $k$  is any constant and  $m_1$  and  $m_2$  are the mass flow rates of the warm upper layer and cold lower layer fluids. Then the peak drawdown fraction is given by,

$$DD_m = \frac{km_1}{m_o} \quad \dots \dots \dots (\text{A.5})$$

Since,

$$\frac{m_1}{m_2} = \frac{h_1}{h_2}$$

for the flume considered here and equating equations (A.4) and (A.5), we have,

$$DD_m = \frac{km_1}{m_o} = \frac{h_1}{h_1 + h_2}$$

# Autoignition of Natural Gas Fuelled Engines -A Review of its Possibilities

**Sii How Sing Masjuki Hassan Mohd. Zaki Abdulmuin**

Department of Mech. Engg. University of Malaya 59100 Kuala Lumpur,  
Malaysia.

## ABSTRACT

This paper outlines a general review of the different possibilities to upgrade Power output and efficiency of conventional natural gas fuelled engines to the diesel fuelled levels. This includes a brief introduction on various aspects and feasible ways of how to achieve "diesel-like" combustion in current natural gas engines. This promises to be an interesting area worthy to be researched for further potential development.

**Keywords :** Autoignition, Natural Gas

## INTRODUCTION

Conventional natural gas fuelled engines have a considerable economic advantage over their diesel and gasoline engines counterparts, and they tend to be technologically innovative and also more environmentally friendly. Natural gas is already chemically ready for use and requires no preliminary treatment. Another advantage of natural gas is its wide flammability limits, especially to the fuel-lean side where ignition of natural gas can occur in the presence of more than 200% theoretical air [1]. Operating in this regime will ensure improved fuel economy and lower emission level. However, this advantage will no longer be enough on its own and may be challenged, and may even decline as a result of the completion for the advanced diesel engines in their next development stage.

As a consequence, the only way natural gas fuelled engines can compete is to improve their shaft efficiencies. This is also because conventional spark-ignition engines technology does not allow the means to achieve "diesel-like" combustion through the direct injection of high-pressure natural gas into the cylinders.

This paper briefly discusses the issue of direct-injection of high-pressure natural gas and a basic study on the various conventional approaches to ignite natural gas, with respect to their possibilities and changes leading to "diesel-like" combustion or autoignition, based on the basis of engineering concerns.

The ramifications of implementing this conceptual development will not only raise the gas engine efficiency and power output, but also the ability to take advantage of future advances in diesel engine technology, such as reducing heat loss through improved combustion chamber insulation.

## **NATURAL GAS**

Basically, natural gas consists of carbon and hydrogen, mainly in the form of methane, CH<sub>4</sub>. Having a simple and stable molecule it is extremely resistant to self-ignite and thus has a low cetane rating. It is also able to mix homogeneously with air to produce a combustible mixture, and is excellent for use in "lean-burn" mixtures which are comparatively less polluting. All these characteristics have made natural gas an intrinsically ecological and environmentally friendly fuel. Therefore, it comes close to the concept of an ideal fuel for this generation and the generations to come.

The octane rating of natural gas is approximately 130, this indicates that sparkignition engines running on natural gas can operate at compression ratios up to 16:1 (normal compression ratios for such engines is between 7.5:1, to 9.5:1) without "spark-knock". Such a tremendous rise in compression ratios will certainly bring about power improvement of 25% to 40% over that of today's low compression gas engines [2].

Being able to achieve a relatively high compression ratio in a natural gas engine is important. The higher ratio causes an increase in thermal efficiency, which in turn reduces fuel consumption. While referring to the general trends revealing the relationship between cetane number, temperatures, fuel type and ignition type shown in the chart generated by Haddad and Watson [3], it was reflected that fuels having cetane number lower than 25 will exhibit a significant feature in ignition delay. Thus it is not hard to perceive that the considerable delay in ignition with natural gas is characterised by its low cetane number.

## **DIRECT-INJECTION IN NATURAL GAS ENGINE TECHNOLOGY**

Power output of the current natural gas fuelled engines, utilizing a carburetted, spark-ignited combustion system (Otto-cycle) is limited by knock of the homogeneous fuel-air charge to approximately 1250 kPa (180 psi) brake mean effective pressure [4].

The knock problem and its related power limitations could be eliminated by directly injecting high-pressure natural gas up to 20000 kPa (3000 psi) into the cylinder near the top dead centre with a gas injection, incorporating ignition assist (glow plug is used) to ignite the low cetane natural gas. And this will produce a "diesel-like" autoignition.

By eliminating the knock limit, the direct-injected gas system can utilize higher compression ratios and higher charge air density than the current gas engines, and furthermore, the flow losses associated with the carburetor will also be avoided. Moreover, the future diesel engine technology improvement

including insulation can be applied to direct-injected gas engines, but cannot be applied to the current gas engines due to knock limitations.

In conjunction with the above, future improvement in the direct-injected natural gas engine, even accounting for the additional parasitic losses associated with increasing the natural gas pressure with a gas compressor is expected to give a significant improvement in net thermal efficiency.

For the direct-injected natural gas engines, special hardware included an electronic gas injector (similar to the diesel's electronic unit injector), a cylinder head incorporating a glow-plug-ignition-assist system and a compressor in the line of fuel supply will all need to be developed to attain a good combustion of the low cetane natural gas fuel.

The Gas Research Institute of Chicago of U.S.A. revealed succinctly in their Annual Report, that natural gas engine power and thermal efficiency comparable to a diesel are achievable by incorporating direct gas injection with glow plug ignition assist (DIG/GPIA) during tests on a Caterpillar 3400 series single cylinder laboratory demonstration engine [a]. The DIGIGPIA system will allow the natural gas engine to have power and thermal efficiency improvement of up to 50% and 137%, respectively, compared to current natural gas engines.

## **HYPERGOLIC SPONTANEOUS COMBUSTION**

Hypergolic combustion is a type of ignition and combustion process, in which fuel and oxidant pair ignites spontaneously and is rapidly combusted. As a result both the ignition delay and the combustion duration of fuel are negligible. For the purposes of this discussion, the phenomenon of hypergolic combustion can be seen to resemble autoignition/spontaneous combustion. Taylor [5] defines autoignition in a fuel-air mixture as a rapid chemical reaction not caused by an external ignition source such as a spark, a flame, or a hot surface.

The hypergolic combustion is a phenomenon which has a promising potential to be applied to a direct-injected natural gas engine. It is aimed at reduction in the ignition delay, improving the quality of combustion, reducing emission levels and increasing overall engine performance.

The primary drawback of most of the listed ignition and combustion alternatives to be discussed in the ensuing section (section 5) revolves around the fact that the bulk of the heat release would be flame speed limited as the flow of natural gas is much slower than gasoline fuel.

Conceptually speaking, the aforementioned problems could be overcome if the natural gas is hypergolically combusted. In another word, prior to injection, if the natural gas is chemically activated, once it is injected it will ignite spontaneously and combustion will occur rapidly. Therefore, if this could be done, the flame speed limitation could be circumvented and the combustion event could be also controlled through the rate of injection. Furthermore, the overall air/fuel ratio and compression ratio could be arbitrarily selected so as to obtain the best trade-off for high efficiency and low emissions.

The basic theory of hypersonic combustion and the experimental results obtained in an engine test fuelled by liquid fuel are presented by Hoppie [6] and Hoppie and Schamweber [2].

Theoretical results prediction speculated by Hoppie [6] indicated that the ignition delay can be made arbitrarily small and essentially independent of air temperature if the fuel is sufficiently preheated.

As demonstrated by Hoppie and Schamweber [7], Hypersonic combustion could be realised in a internal combustion engine by means of preheating the fuel. The reduction in ignition delay and increase in combustion rate will result, in conjunction with fuel injection rate and duration control would provide much better control of the combustion event. Therefore, following this, the engine power output, emission levels and engine efficiency can be optimised.

With reference to the above arguments, one can propose that thermal energy can be used as a means of activating the fuel, i.e., as a means to produce fuel radical such as;  $\text{CH}_4$  to  $\text{CH}_3$ ,  $\text{CH}_2$ ,  $\text{H}$ , etc.

In the midst of optimism, engineering problems in handling high temperature fuel must not be ignored and it needs to be resolved before the idea of hypersonic combustion can become practical and technically viable.

## IGNITION AND COMBUSTION ALTERNATIVES

In combustion, the "reaction" is not a single or even a few-step Process; the actual chemical mechanism consists of a large number of simultaneous, interdependent reactions or chain reactions. In such chains there is an "initiating reaction" where highly reactive intermediate species or radicals are produced from stable molecules, i.e., from fuel and air. This is then followed by propagation reactions radicals react with the reactant molecules to form products and other radicals to continue the chain, Heywood [8].

This section presents the possible alternative approaches, having potential to start "initiating reaction", in which more effort is required to evaluate and investigate both theoretically and experimentally each scheme's possibility in leading to "diesel-like" combustion for natural gas engine.

### Thermal Energy Activation

The mathematical model developed by Hoppie [6], which predicts that ignition delay is a function of fuel and air temperature, implies that the concentration of chemically active fuel radicals can be significantly increased via thermal dissociation of the fuel by preheating it. Therefore, if the fuel is so activated, it will ignite and be consumed much more rapidly upon injection into cylinder than through fuel injected at ambient temperature.

A major anticipated shortcoming, associated with thermal activation is the fact that there is a tendency of coke formation if fuels are held at high temperatures for long duration time due to coking. Compression heating could be possible to minimise the occurrence of coke

formation. Using the process of compression heating, i.e. through rapid compression, it is conceivable that the desired radicals could be created and injected prior to the coke formation. Another practical way of eliminating coke formation is through the addition of water to the gas prior to heating.

### **Catalytically Enhanced Thermal Energy**

This criterion is based on the fact that upon employment of some suitable catalyst, chemical reactions can be forced to occur at a temperature lower than normally expected. This is also a practical way to generate fuel radicals at a temperature just low enough to avoid the formation of coke. Other advantages of this scheme are the provision of a sustained combustion with lean mixture and also low pollutant product, owing to more complete combustion.

There are two possible means of modifying natural gas in order to achieve autoignition, and hence combustion, without assistance upon injection into an engine. They are (i) catalytic activation of natural gas and (ii) catalytic activation of natural gas and air. The basic idea behind catalytic enhancement of natural gas rests on the fact that a suitable catalyst can create certain chemical species or active radicals, at a lower temperature than normally would be required if no catalyst is present. Some potential catalysts are MgO, metallic nickel, both alpha and gamma phase  $Al_2O_3$  and  $SiO_2$ . This can be accomplished by the introduction of an in-line catalyst chamber at the inlet of the fuel line, in which contains the pelletized catalytic materials.

### **Partial Catalytic Combustion**

This concept has been developed in the Jet Propulsion Laboratory and Siemens of U.S.A., Houseman and Cerini [10]. Their idea is to improve liquid-fuelled sparkignited engines by first converting the liquid fuel into a hydrogen-rich gas, in other words, such a fuel would offer improved efficiency and lower emissions. To convert to a hydrogen-rich gas, the liquid fuel was first vaporized, mixed with a small amount of air, and then allowed to partially combust with the aid of and in the presence of a suitable catalyst. It was found that this could be accomplished without coke formation, and that the product gas was rich in fuel radicals and atomic hydrogen, at an approximate temperature of 66 degree Celsius (150 degree F). This product gas would be directly injected into the engines to achieve autoignition, which is the concept of hypergolic combustion.

### **Compression Ignition**

In this concept, compression combustion via preheated inlet air can occur without relying on any external source of ignition in a direct-injected natural gas engine. Having a very low cetane rating compression ignition of natural gas is quite difficult to achieve in a conventional diesel engine without

modification of the engine. However, conventional compression ignition can be accomplished via preheated inlet air. This is a very promising method leading to hypergolic combustion. In this case, waste heat given out by engine can be harnessed to preheat the inlet air, either through heat-exchange from cooling system, lubrication system or exhaust system.

### **Electrical Energy Ignition**

Theoretically, the establishment of an electric discharge in the natural gas will generate radicals. This may be done by utilizing a corona or an arc discharge. One can anticipate that, even through direct injection of natural gas, spontaneous ignition is still far from reality. The actual heat release would most probably result from flame propagation, which is predicted on the establishment of a sufficiently large flame kernel resulting from the interaction of a rather small portion of the injected fuel with the ignition source. Due to the excessively long combustion duration, low efficiency and high emission could thus be expected.

If methane or natural gas is electrically activated with an arc discharge during injection, negligible ignition delay and rapid combustion are possible. Theoretically, this offers a great practical value. With proper amount of electrical activation, a controlled combustion event could be achieved with accompanying low levels of emission.

### **Photochemical Dissociation**

Prior to injection, an ultra violet source could be employed to activate methane by projecting an ultra violet beam into a portion of natural gas to establish chemically active, unstable fuel radicals from stable molecules to enhance the vigour of the combustion.

### **Pilot Injection**

Pilot injection of diesel fuel as a primary means of providing a flame kernel is predicted to be sufficient to ignite directly injected natural gas. However, the profile of flame front for combustion of the gas is the main parameter to control the efficiency and emissions output.

### **Glow Plug Ignition**

A glow plug appears to be quite promising in leading to autoignition in natural gas. It is very similar to a liquid-fuelled, directed, spark-ignited engine or a spark-assist diesel engine.

### **Plasma Jet Ignition**

The concept in this particular type of ignition scheme is borrowed from the technology of the torch ignition engine, in which, charge separation may be achieved by using a pre-chamber for a rich mixture

of fuel and air and the main chamber for a weak mixture. The injection system can be used to supply fuel, Benson and Whitehouse [11]. By the creation of a plasma jet of fuel (diesel fuel or just natural gas), or air or both air and fuel in a prechamber, while injecting natural gas into the combustion chamber, natural gas will be ignited by the impingement and interaction with the second jet, i.e., the plasma jet. This ensuing plasma jet is rich, consisting of chemically active species and would create a vigorous reaction within the primary fuel/ air mixture. This plasma jet can be attained via electrical discharge in air, fuel, or air/fuel. Under this phenomenon, combustion duration can be greatly reduced, hence, improved combustion process will result.

### **Laser Ignition**

Instead of using electrode spark plug, a laser beam can be utilised to introduce an intense electric field breakdown in the combustion chamber to ignite the natural gas as it is injected. In this case, a laser beam is focused inside the combustion chamber to create a region of such intense electric field that breakdown of the stable species of fuel occurs.

### **CONCLUSIONS**

Based on hypergolic combustion, a direct ignition incorporating glow-plug ignition-assist system, the dream of achieving 'diesel like' performance in a conventional natural gas engine is viable through the means of activation of natural gas as mentioned above. This will not only result in improved power output and thermal efficiency, it also permits the natural gas engine to take full advantage of future advanced diesel engine improvements such as the application of ceramic liner for combustion chamber insulation. With the advent of the technology, low heat rejection diesel engine natural gas as an alternative fuel has become possible offering the advantages of burning low cetane fuel.

With hypergolic combustion, the combustion event will be completely different from that of spark-ignition or compression-ignition, hence, it is logical to suspect that the injected fuel pattern, heat transfer profile and thus the combustion shape itself should be different.

At this stage, sufficient data are not available to further determine and compare as to which concept/scheme is superior from the engineering point of view.

### **RECOMMENDATIONS**

1. Each of the scheme / approach as well as their amalgam of different schemes or 'hybrid' system consisting of the combination of the above mentioned schemes should be experimentally evaluated to determine if they are technically viable to achieve autoignition in the natural gas engine
2. Improved air turbulence is likely to provide the desired improvement in combustion.

3. As natural gas has high resistant to 'spark-knock', therefore, high compression ratios can be attempted, giving high thermal efficiency, similar to the comparable diesel engine, which in turn reduces the fuel consumption.
4. Multiple plugs with different configurations can be tried on the diameter of each cylinder to achieve optimal combustion rates, and leading to higher efficiency.
5. Generally, a three-way catalytic converter can be fitted to a natural gas engine to cut down the amount of carbon dioxide, carbon monoxide, oxides of nitrogen and nonmethane hydrocarbons in the exhaust emission.
6. By the use of a small prechamber with each cylinder that burns a rich mixture of natural gas and air, which is ignited by a spark plug, and on the other hand, the main portion of the combustion chamber burns a lean mixture, which is ignited by the burning gases in the prechamber, combustion will occur at lower temperatures than usual. Thus reduction of the nitrogen oxides could be achieved.

## REFERENCES

1. Crane, M.E. and King, S.R., *Emission Reductions Through precombustion Chamber Design in a Natural Gas, Lean Burn Engine*, Transactions of the ASME, Vol. 714, pp. 446-452, July 1992.
2. *Natural Gas Training Manual*, British Columbia Institute of Technology, pp. 9, 1991.
3. Haddad, Sam and Watson, Neil, *Principles and performance in Diesel Engineering*, Ellis Horwood Limited, pp. 59-60, 1984.
4. Richards, G., *Direct Gas Injection with Glow Plug Ignition*, Gas Research Institute, Annual Report, GRI-88/0271, 1988.
5. Taylor, C.F., *Internal Combustion Engine in Theory and Practice*, The M.I.T. Press, pp. 43, 1966.
6. Hoppie, L.O., *The Influence of Initial Fuel Temperature on Ignition Delay*, SAE Paper No. 820356, 1982.
7. Scharnweber, D.H. and Hoppie, L.O., *Hypergolic Combustion in an Internal Combustion Engine*, SAE Paper No. 850089, 1985.
8. Heywood, J.B., *Internal Combustion Engine Fundamentals*, McGraw-Hill International Editions, pp. 462-464, 1988.
9. Strehlow, R.A., *Combustion Fundamentals*, pp. 778, 248, 408, 1985.
10. Houseman, J. and Cerini, D., *On-Board Hydrogen Generator for a partial Hydrogen Injection Internal Combustion Engine*, SAE paper No. 740600, 1974.
11. Benson, R.S. and Whitehouse, N.D., *Internal Combustion Engines*, Pergamon Press, pp. 22, 1979.

# Computation Studies of Air Flow in Two Dimensional Coaxial Pipe

**Adi Surjosatyo and Farid Nasir Ani**

Fakulti Kejuruteraan Mekanikal Universiti Teknologi Malaysia 81310 UTM  
Skudai, Johor DT, Malaysia

## ABSTRACT

The present study conducted a computer simulation of a turbulent flow in a two coaxial pipes with varying pipe diameter and entrance displacement (AL). The entrained flow characteristics together with the effect of the temperature of the entrained flow inlet were studied with variation of AL. The numerical method employs differencing scheme for integrating the continuity equation and energy equation. An equation k-e turbulent model was used to simulate the turbulent transport quantities. A Fluent CFD package was used to produce 2-D predictions of the flow pattern. Results show that increasing the air entrained temperature until 600 K will decrease the air flow rate and the diameter ratio of 2.0 has the highest entrained flow rate.

**Key words:** Coaxial pipes, k-e turbulent model, CFD modeling, 2D flow, entrance displacement, air ejector.

## INTRODUCTION

Ejectors are apparatus which entrained the low pressure gas by high pressure gas interchanging the momentum of high speed driving gas discharged through a nozzle (or nozzles) with momentum of low pressure entrained gas, forming jet (or jets). Ejectors usually consist of a nozzle (or nozzles) and a diffuser. That is, it has no moving part such as a rotor or piston. One of the merits of ejector is that it is simple in construction and it could compress a large flow rate of driving gas for the small and simple size ejector design as shown on Figure 1.

There are other names for the system which have the same working principles, such as jet pump, injector and eductor. The general name for these systems is jet apparatus. The names above mentioned are distinguished according to the kinds, states and properties such as compressibility (gas, liquid, mixture of liquid and solid) of the driving and entrained fluids. Based on the usual ejector design the present study is to propose some data for the design of the subsonic air in a coaxial pipe configuration.

A research on ejector by Johannesen (1951) reported that the features of ejector driven by and entraining compressible fluids. These include the aerodynamics of flow in the actuating nozzle, mixing chamber and the supersonic and subsonic diffusers. In general, the emphasis are made on the steam driven air ejector and experiments were under on such ejector; covering a range of geometrical proportions and pressure ratios.

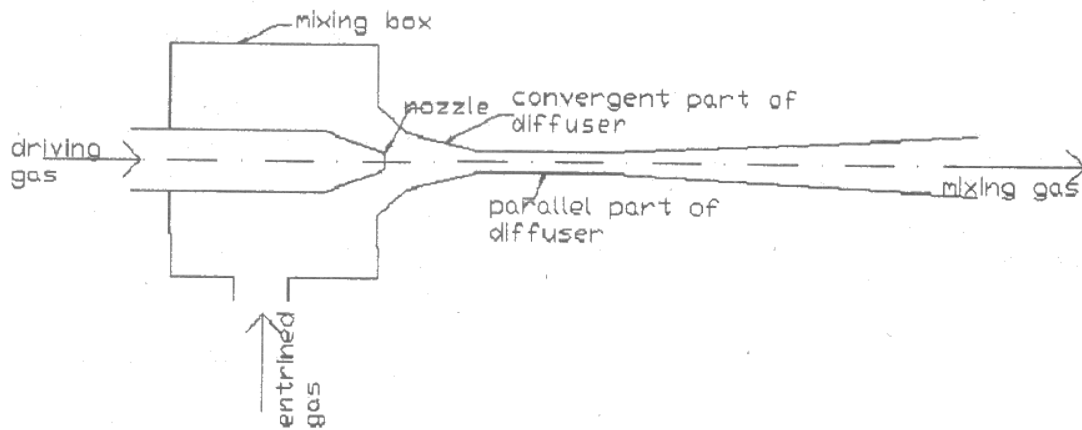


Figure 1. Ejector configuration

A one dimensional method of analysis of air ejector is presented by Keenan et al, (1950). The analysis considers mixing of the primary and secondary streams at constant pressure and constant area and it is concluded that better performance will result from constant pressure mixing. It should be noted, however, that while experimental verification of the analysis constant area is good, the lack of a suitable design of constant-pressure mixing chamber has prevented from demonstrating the calculated supremacy of this ejector design.

There are many of the previous paper deal with single and multiple nozzle ejector, In the implementation of these design should have a high air compression (2 bars) to have a sufficient entrained air. In the present work it will be developed by another type of a simple ejector in the form a pair of coaxial pipe which has a purpose to work on low air compression (2 bars). The present study is objected to so-called an ejector which deals with compressible gases as the driving gas and entrained gas. One of the merits is that it could use a blower with low power and entrained gas could occur which matches a specially fixed application.

## THE AIR EJECTOR MODEL

Figure 2 shows the air flow and configuration of the coaxial pipes. The primary air or driving air is introduced into the inlet pipe I which acts as nozzle function, It is to be expected due to pressure drop at outlet pipe I occur the entrained air flow in pipe II which acts as diffuser function.

In this model the length of driving pipe or pipe I is 665 mm and the length of entrain ejector pipe is 650 mm. The pipe entrance displacement start from from  $AL=50$  mm (0.050 m) and it increased until  $AL=420$  mm (0.420 m). Diameter Ratio (DR) means here the diameter ratio of entrain ejector pipe to the drive pipe. The different size of entrain ejector diameter are varied while the drive pipe diameter is constant. The Diameter Ratio (DR) variation are 1.63, 2.34, 2.62 and 2.81. In this model is assumed that there is no friction on the surface pipe. Therefore the calculation regarding to the wall roughness is negligible.

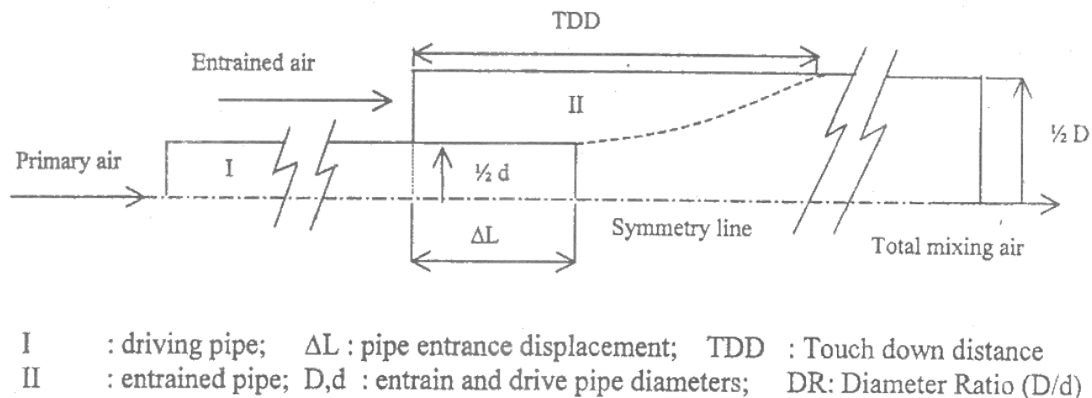


Figure 2. Air flow and ejector - drive pipes

## GOVERNING EQUATIONS

The physical model considered in this work are shown schematically in Figure 2. This configuration is a two dimensional of co-axial pipe with turbulent flow in the two pipes. The governing Reynolds-averaged equations for steady-state turbulent flow of twodimensional (Fluent User's Guide, 1997; Shaw, 1998; Patankar, 1980) are as followed:

### Continuity Equations:

a. incompressible fluid:

$$\frac{\partial U}{\partial X} + \frac{\partial V}{\partial Y} = 0 \quad (1)$$

b. compressible fluid:

$$\frac{\partial \rho}{\partial t} + \frac{\partial (\rho U)}{\partial X} + \frac{\partial (\rho V)}{\partial Y} = 0 \quad (2)$$

### Momentum Equations:

$$\begin{aligned} \rho \frac{\partial U}{\partial t} + \rho U \frac{\partial U}{\partial X} + \rho V \frac{\partial U}{\partial Y} = -\frac{\partial P}{\partial X} + \frac{\partial}{\partial X} \left( \nu \frac{\partial U}{\partial X} \right) + \frac{\partial}{\partial Y} \left( \nu \frac{\partial U}{\partial Y} \right) + \\ \text{a. } \frac{\partial}{\partial X} (-\overline{u'u'}) + \frac{\partial}{\partial Y} (-\overline{u'v'}) \end{aligned} \quad (3)$$

$$\begin{aligned} \rho \frac{\partial V}{\partial t} + \rho U \frac{\partial V}{\partial X} + \rho V \frac{\partial V}{\partial Y} = -\frac{\partial P}{\partial Y} + \frac{\partial}{\partial X} \left( \nu \frac{\partial V}{\partial X} \right) + \frac{\partial}{\partial Y} \left( \nu \frac{\partial V}{\partial Y} \right) + \\ \text{b. } \frac{\partial}{\partial X} (-\overline{u'v'}) + \frac{\partial}{\partial Y} (-\overline{v'v'}) \end{aligned} \quad (4)$$

The two equations, Eq. (3) and (4) derived from Newton's Second Law, describe the conservation of momentum in the flow also known as the Navier-Stokes equations. The terms on the left-hand side of each of these equations describe acceleration term, the second and third terms being the convection terms, then the right hand side terms come from the pressure gradient in the flow and the effects of viscosity and the last two terms that so called the Reynold stresses represent the model to account for the effects of turbulence. These momentum equation governs the time-averaged properties of the flow.

### The turbulence Models

To solve Equations (1) to (4), a turbulence model for the turbulent transport quantities has to be specified. In the present work, the standard k-ε model (Fluent user's Guide, 1997; Shaw, 1998; Launder and Spalding, 1972) based on Boussinesq hypothesis is adopted. The local mean state of turbulence can be characterized by the turbulent kinetic energy  $k$  and its dissipation rate  $\epsilon$  according to:

$$\rho \overline{u_i' u_j'} = \rho \frac{2}{3} k \delta_{ij} - \nu \left( \frac{\partial u_i}{\partial x_j} + \frac{\partial u_j}{\partial x_i} \right) + \frac{2}{3} \nu \frac{\partial u_i}{\partial x_i} \delta_{ij} \quad (5)$$

where

$$k = \frac{1}{2} \sum_i \overline{u_i'^2} \quad (6)$$

$$\nu = \rho C_{\nu} \frac{k^2}{\epsilon} \quad (7)$$

$$\epsilon = k^{2/3} / l_{\epsilon} \quad (8)$$

### Transport Equation For K And ε

The values of  $k$  and  $\epsilon$  Equation (7) are obtained by solution of conservation energy:

$$\frac{\partial}{\partial t}(\rho k) + \frac{\partial}{\partial x_i}(\rho u_i k) = \frac{\partial}{\partial x_i} \left( \frac{\nu}{\sigma_k} \frac{\partial k}{\partial x_i} \right) + G_k + G_b - \rho \epsilon \quad (9)$$

$$\frac{\partial}{\partial t}(\rho \epsilon) + \frac{\partial}{\partial x_i}(\rho u_i \epsilon) = \frac{\partial}{\partial x_i} \left( \frac{\nu}{\sigma_{\epsilon}} \frac{\partial \epsilon}{\partial x_i} \right) + C_{1\epsilon} \frac{\epsilon}{k} (G_k + (1 - C_{3\epsilon}) G_b) - C_{2\epsilon} \rho \frac{\epsilon^2}{k} \quad (10)$$

where

$$G_k = \nu \left( \frac{\partial u_j}{\partial x_i} + \frac{\partial u_i}{\partial x_j} \right) \frac{\partial u_j}{\partial x_i} \quad (11)$$

$$G_b = -g_i \frac{\nu}{\rho \sigma_h} \frac{\partial \rho}{\partial x_i} \quad (12)$$

### The Effects of Turbulence on Heat Transfer

When the heat is added to a fluid and the fluid density with temperature flow can be induced due to the force of gravity acting on the density variations. Such flows are termed natural-convection (mixed-convection) flows. The importance of buoyancy forces in a mixed convection flow can be measured by the ratio of Grashof and Reynolds number:

$$\frac{G_r}{R_e} = \frac{\Delta \rho g h_c}{\rho v^2} \quad (13)$$

When this ratio approaches or exceeds unity, the flow should have a strong buoyancy to the flow (Fluent User's Guide, 1997).

In this simulation, there are some correlation between the turbulence flow and the fluid flow temperature. This correlation is based on the momentum equation and again the Boussineq model is adopted. For simplifying the momentum equation, it will perform the flow in y-direction (Shaw, 1989):

$$\frac{\partial V}{\partial t} + U \frac{\partial V}{\partial X} + V \frac{\partial V}{\partial Y} = -\frac{1}{\rho} \frac{\partial p}{\partial Y} + \frac{\mu}{\rho} \left( \frac{\partial^2 V}{\partial X^2} + \frac{\partial^2 V}{\partial Y^2} \right) + g\beta(T - T_f) \quad (14)$$

Another theoretical correlation is based on the conservation of energy which can predicted the heat transfer process within the fluid and/or within solid in the model (Fluent User's Guide, 1997). The simulation model solve the energy equation in the form of a transport equation for the static enthalpy, h:

$$\frac{\partial}{\partial t}(\rho h) + \frac{\partial}{\partial X_i}(\rho u_i h) = \frac{\partial}{\partial X_i}(k_c + k_t \frac{\partial T}{\partial X_i}) - \frac{\partial}{\partial X_i} \sum_j h_j J_j + \frac{\partial p}{\partial t} + \tau_{ik} \frac{\partial U_i}{\partial X_k} + S_h \quad (15)$$

Enthalpy h defined as:

$$h = \sum_j m_j h_j \quad (16)$$

$$\text{where: } h_j = \int_{T_{ref}}^T c_{p,j} dT$$

## NUMERICAL METHOD

The commercial software package, Fluent version 4.4, produced by Fluent Inc. was used as the primary source code for the model. This package employs a control volume-based, finite difference solution technique to allow full characterization of the flow field. The Reynolds-averaged Navier-Stokes equations coupled with the Reynolds-averaged governing differential equations of continuity, energy, and species are solved in a discretized form. The standard k-ε turbulence model is employed. To obtain values at control volume interfaces needed for flux calculations, the power law interpolation scheme is utilised. The pressure-linked continuity and momentum equations are solved using the Semi-Implicit Method for Pressure-Linked Equations Consistent (SIMPLEC) solution algorithm. Specific details regarding convergence parameters such as multi-grid and under relaxation factors are available in

Fluent. The convergence criterion is specified as the relative difference of every dependent variable between iteration steps being smaller than  $10^{-6}$ . The pipe form in the present work is assumed as circular form.

## CONDITIONS OF SIMULATION

Simulations of subsonic air ejector was done according to obtain an optimum condition of air flowrate in a pair of coaxial pipe. The simulations are being carried out using a CFD software package. The conditions of simulation are as follows:

- subsonic and compressible air flow
- turbulence method: k-  $\epsilon$  method
- boundary conditions:
  - i) inlet pressure as primary air at inside-pipe: 2 bars,
  - ii) inlet pressure where the secondary air or entrance air is induced: 1 bar (atmospheric pressure),
  - iii) inlet pressure at the outlet pipe where the exit of total air flow takes place: 1 bar (atmospheric pressure),
- 2 D flow analysing.

## RESULTS AND DISCUSSIONS

### Effect of Variation of Diameter Ratio on Air Velocity and Air Flowrate

Figure 3 to Figure 4 show the graphs of air velocity (AV) and air flowrate (AF) versus diameter ratio. Each of the Figures has two types of curve, namely, primary (driving air) and entrained air flow. For primary air flow is kept constant. The displacement of entrance pipe has not much influence to the primary air flowrate curve due to the pressure intake is high enough compared to the pipe resistance, but for the entrained air flow there is a reduce both for air velocity and flowrate. The increasing of pipe displacement means increasing of flow path. Therefore the area of entrained air flow is more restricted. It means the flow path for the entrained air has more resistance. From the graph that the highest entrained air flow is achieved at 0.05 m where this distance is on the first drive pipe displacement.

Figure 5 and 6 show the effect Diameter Ratio variation on entrained air flowrate. Figure 5 plotted curves in which the increasing of DR has caused the entrained mass flowrate also increased.

To describing both of these conditions it is necessary the continuity equation is to be implemented:

$$\frac{\partial}{\partial t} \int \rho dv + \int \rho v \cdot dA = 0 \quad (17)$$

Assumed the flow is steady, therefore the first term is zero ( $\frac{\partial}{\partial t} \int \rho dv = 0$ ), hence:

$$\int \rho v \cdot dA = 0 \quad (18)$$

Since there is no flow through the wall and the flow is compressible, the equation (18) changed into:

$$\rho_1 V_1 A_1 = \rho_2 V_2 A_2 = m \quad (19)$$

According to the Equation (19), when DR increase means the area of flow is also increase, so the volumetric flow rate  $m$  is also increase as in Figure 5 and air flow velocity is decreased as shown in Figure 6,

### **Effect of Diameter Ratio and Drive Pipe Displacement on Touch Down Distance (TDD)**

Figure 7 and 8 show the graphs of the effect of both diameter ratio and drive pipe displacement (AL) on Touch Down Distance (TDD). In these graphs three curves were plotted, Diameter Ratio (DR) 1.63, 2.34 and 2.62 have created the touch down distance, except for the highest displacement LL 0.420 m, In this displacement there is no touch down point on the entrain pipe and it has created turbulence effect on the outlet section of the entrain pipe since TDD is beyond the length of the pipe. Consequently, this condition could cause a flow resistance. The TDD have a tend to increase for higher DR. Figure 7 show the smallest TDD is achieved by the smallest displacement. Also increasing the entrance displacement the TDD increased also as in Figure 8, It should be that there is a correlation between the entrained mass air flowrate and TDD. It means the entrained flow path, since it is affecting reduction of the mass air flowrate, influence the TDD significantly.

Graphs show that higher DR could influence higher entrained mass and increasing of this mass flowrate 'has affected TDD to increase flowrate as in Figure 7. Due to the DR variation has a correlation with flow area which has influenced mass air flowrate, thus it could be deducted the flow area is a factor which has also influenced TDD. Graphs on Figure 8 show that higher AL has increased TDD. It means that TDD is affected by air flow path between the drive pipe and entrain pipe.

**Effect of Variation of Gas Temperature on Entrained Air Flowrate and Air Velocity** Figure 9 to Figure 12 show graphs of entrained air flowrate and air velocity at different ambient temperature of the inlet secondary pipe (entrance pipe). These figures show that the increasing of air temperatures of 300, 500 and 600 oC at different Diameter Ratio DR of 1.63, 2.34, 2.62 and 2.81 which have influenced the

variation of air flowrate and velocity. The increasing of gas temperature affected the increasing the entrained air velocity, but there is a decreasing of entrained air flowrate.

The properties of air at atmospheric pressure (Holman, 1993) are listed in tables i.e, value of air density and specific heat which are correlated with different air temperature. Increasing of air temperature affect the decreasing of air density and increasing of specific heat, There is a correlation at the gas law (Streeter, 1983; Fluent User's Guide, 1997; Holman, 1993) between air density and the temperature as follow:

$$\rho = p_{op}/RT_a \quad (20)$$

If the temperature increase, the air density should be decrease. Based on the continuity equation, namely, Equation 19 the decreasing of density affected the air flowrate, it means the air flowrate is decreased. Another explanation is based on energy equation as in Equation 16. Increasing the air temperature is effecting the increment of specific heat capacity value  $c_p$  (Cengel, 1999). To balancing the total heat capacity of the system the mass flowrate should decrease.

Increasing of the temperature effecting also the air velocity. When the system changes from some initial velocity  $v_1$  to a velocity  $v_2$ , the corresponding change in kinetic energy is (Holman, 1993):

$$\Delta E = KE_2 - KE_1 = \int_{v_1}^{v_2} \frac{m}{g_c} v dv = \frac{1}{2g_c} m (v_2^2 - v_1^2) \quad (21)$$

The conservation energy shows that when the temperature in a system is increasing then the heat  $Q$  in the system increase also. It means there is a change in the internal energy  $\Delta E$ . The work  $W$  is altered according to the conservation energy by the amount of heat energy added  $Q$ , thus:

$$Q + W = \Delta E \quad (22)$$

It indicates that

Energy added to system = accumulation of energy in the system.

At the present work there is no work  $W$  or  $W = 0$ , thus Equation 22 becomes

$$Q = \Delta E \quad (23)$$

$$\text{where } Q = h_i = \int_{T_{ref}}^T c_{p,i} dT.$$

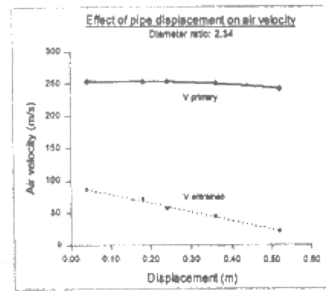


Figure 3

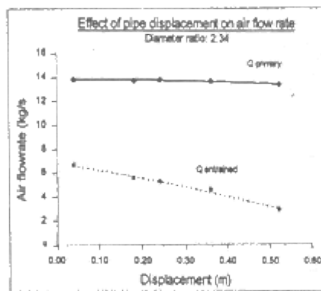


Figure 4

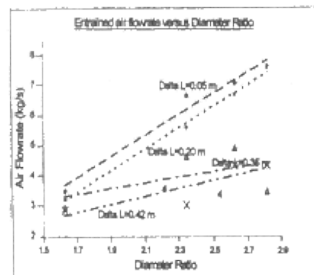


Figure 5

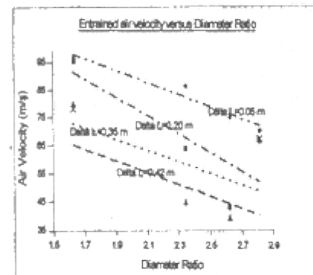


Figure 6

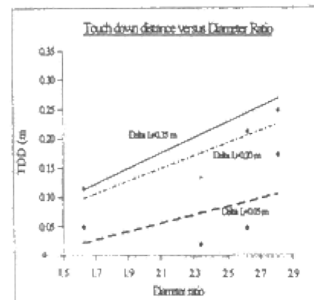


Figure 7

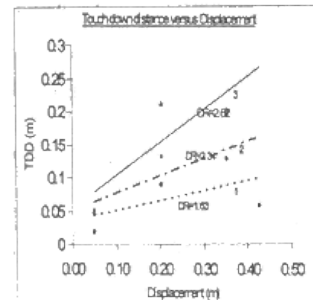


Figure 8

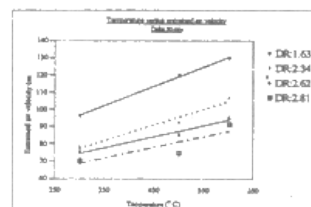


Figure 9

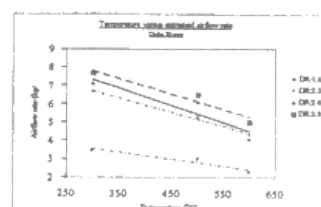


Figure 10

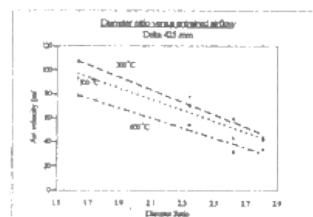


Figure 11

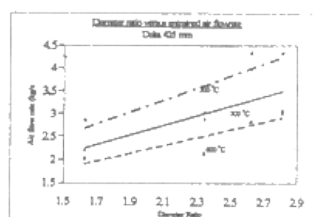


Figure 12

## CONCLUSIONS

2-dimensional cold-flow simulations have been performed for the model geometry of coaxial pipes, It was demonstrated that the variation of drive pipe diameter and entrance pipe displacement did play a major role of entrained mass flow rate and Touch Down Distance. Flow simulations result show that the Diameter Ratio of 1.63 has the smallest flow area, as the consequence, there is the lowest entrained air flowrate, For each diameter ratio increasing of Diameter Ratio will increase the air flowrate, but the

entrance pipe displacement will decrease the entrained rate. It has indicated that there is a correlation between entrained mass flow rate and Touch Down Distance. Thus, if the entrained air flow is low then Touch Down Distance is short, The result also indicate that Touch Down Distance is influenced by two conditions i.e., displacement due to pipe resistant, and diameter ratio as well as flow area which has relationship with mass air flowrate,

The gas law and energy conservation law are important equations to explain the correlation of air velocity and air flowrate with the variation of gas temperature. Increasing the temperature until 600 K will decrease the air flow rate and the diameter ratio of 2.81 has the highest entrained flowrate.

## NOMENCLATURE

$A$	inflow area, $m^2$
$C_{v1}$	constant of proportionality (= 0.09)
$C_{1e}$	empirical constants (=1.44)
$C_{2e}$	empirical constants (=1.92)
$dv$	element of volume, $m^3$
$h_c$	average heat transfer coefficient, $W/m^2\ ^\circ C$
$i, j$	direction of flow, -
$g$	standard gravity acceleration (= $9.807\ m/s^2$ )
$g\beta(T-T_f)$	additional term for buoyancy
$J_j'$	diffusion flux of the species $j'$
$G_k$	the rate of production of turbulent kinetic energy, $kg/m\ s^3$
$G_b$	generation of turbulence due to buoyancy, $kg/m\ s^2$
$G_r$	Grashof number
$k$	turbulent kinetic energy, $m^2/s^2$
$k_0$	molecular conductivity, $W/m\ ^\circ C$
$k_t$	effective conductivity due to turbulence transport ( $k_t=c_p\mu_t/Pr_t$ )
$l_e$	mixing length scale, $m$
$\dot{m}$	volumetric flow rate, $kg/s$
$P$	mean pressure, $Pa$
$P_{op}$	operating pressure, $Pa$
$R$	gas constant, $8.31434\ kJ/kmol\ K$
$Re_c$	Reynold number, -
$S_h$	term including heat of chemical reaction, any interphase exchange of heat, any other volumetric heat sources, -
$T_a$	ambient temperature, $K$
$T_f$	Temperature reference, $K$
$t$	velocity flow time, $s$
$U, V$	mean velocity components in the direction of (X,Y), $m/s$

$v$	inflow velocity, m/s
$u', v'$	fluctuating components velocity in the direction of (X,Y), m/s
$\beta$	coefficient of volume expansion, 1/K $= \frac{1}{v} \left( \frac{\partial v}{\partial T} \right)_p = - \frac{1}{\rho} \left( \frac{\partial \rho}{\partial T} \right)_p$
$\overline{u'u'}$	Reynold stresses, $m^2/s^2$
$\overline{u'v'}$	Reynold stresses, $m^2/s^2$
$\overline{v'v'}$	Reynold stresses, $m^2/s^2$
$\rho$	density, $kg/m^3$
$\delta_{ij}$	wall shear layer thickness, m
$\sigma_k$	"Prandtl" numbers governing the turbulent diffusion of k and $\epsilon$ , (=1.0)
$\sigma_\epsilon$	Prandtl numbers governing the turbulent diffusion of k and $\epsilon$ , (=1.3)
$\mu$	turbulent viscosity is proportional to the product of a turbulent velocity scale and length scale, $N.s/m^2$
$\nu$	kinematik viscosity, $m^2/s$
$\epsilon$	distribution of dissipation rate of k, $m^2/s^3$

## ACKNOWLEDGMENT

The authors are grateful to RMC (Research Management Center), UTM for supporting the fund to this research.

## LITERATURES

- 1.Yamamoto, F., Performance of Subsonic Air Eiector with multiple nozzles, Memoires of The Faculty of Engineering, Fukui University, Vol. 30 No.1 1982.
- 2.Streeter, Y.L., Fluid Mechanics, McGraw-Hill International Book Company, 1983.
- 3.Fluent User's Guide, Fluent 4.4, Yo1. 1, 3 and 4, May 1997 .
- 4.Holman, J.P ., Thermodynamics, McGraw-Hill Intemational Book Company, 1993
- 5.Johannesen, N.H, Ejector theory and experimenrs, Danish Acad. Tech. sci. No. 1.176p(1951)

6. "Thermophysical Properties of Matter - An Introduction to combustion", 1993.
7. Keenan, L. H., Neumann, E.P. and Lustwerk, F.p., An investigation of ejector design by analysis and experiment J. Appl. Mech., 17, 3 ( 1950).
8. Shaw, C. T, Computational Fluid Dynamic, Longman, 1999.
9. Panton, R. L., Incompressible Flow, John Wiley & Sons, 1994.
10. Patankar, S. Y., Numerical Heat Transfer and Fluid Flow, Hemisphere publishing Corporation, 1980.
11. Launder, B. E., and Spalding, D. B., Lectures in Mathematical Models of Turbulence, Academic Press, London, England, 1972.
12. Hwang, R. R. and Chow, Y. C., Computation of turbulent flow over two dimensional surface-mounted rib, proceedings of the 6th Flow Modelling and Turbulence Measurements, Florida, 1996.
13. Cengel, Yunus, Heat Transfer: A practical Approach, McGraw Hill, 1998.

# A Classical Generalized Variational Principle for Pseudo-State Thermoelasticity of Piezoelectric Materials

**Ji-Huan He**

Shanghai University, Shanghai Institute of Applied Mathematics and Mechanics,  
149 Yanchang Road, Shanghai 200072, People's Republic of China

## **ABSTRACT**

It is very difficult to establish a classical variational Principle (not Gurtin-type not involving convolutions) for thermopiezoelectricity. However, the semi-inverse method proposed by He appears to be one of the best and most convenient ways to establish variational principles for the physical problems. By such method, a classical generalized variations has been established for the Pseudo-static thermoelasticity of piezoelectric materials.

**Keywords:** Variational Theory, Semi-inverse Method, thermopiezoelectricity

## **INTRODUCTION**

Recent interest in piezoelectric materials stems from their potential applications in intelligent structural systems. A comprehensive list of works in this area may be found in [1~4] and the references cited thereby. The rapid development of computer science and the finite element applications reveals the importance of searching for a classical variational principle for the thermopiezoelectricity, which is the theoretical basis of the finite element methods [5] and meshfree methods [6].

## **A GENERALIZED VARIATIONAL PRINCIPLE**

Though it is easy to establish a Gurtin-type functional (involving convolutions), it is very difficult to construct a classical variational model due to the strongly coupled constitutive relations and the terms of the first-order time-derivatives involving in the heat conduction equation. As the author knows, there exist no such classical variational models for the thermopiezoelectricity, the semi-inverse method [6~9] that we are proposing appears to be one of the best and most convenient ways to establish variational principles for the physical problems. By such method we obtained following generalized variational principle with 9 kinds of independent variations (stress  $\sigma_{ij}$ , strain  $\gamma_{ij}$ , displacement  $u_i$ , temperature  $\theta$ , heat flux  $q_i$ , electric displacement  $D_i$ , electric field  $E_i$ , electric potential  $\Phi$  and entropy  $S$ )

$$J(\sigma_{ij}, \gamma_{ij}, u_i, \theta, q_i, D_i, E_i, \Phi, S) = \int_{t^{(n-1)}}^{t^{(n)}} \int L dV dt + IB$$

where

$$\begin{aligned} L = & \sigma_{ij} \gamma_{ij} - \frac{1}{2} \sigma_{ij} (u_{i,j} + u_{j,i}) \\ & + \gamma_{ij} \left( -\frac{1}{2} a_{ijkl} \gamma_{kl} + e_{mij} E_m + b_{ij} \theta \right) + f_i u_i \\ & + \theta \left( \frac{1}{2} c \theta_0 \theta + c_i E_i - t' q_{i,i} - \alpha \right) \\ & + \frac{1}{2} (K_{ij} \tau + t') q_i q_j - \beta q_i - E_i D_i + \frac{1}{2} E_i \varepsilon_{ij} E_j + D_i \Phi_{,j} \\ & + \lambda (\rho S - c \theta - b_{ij} \gamma_{ij} - c_i E_i)^2, \end{aligned}$$

$$\begin{aligned} IB = & \int_{A_1} \sigma_{ij} n_j (u_i - \bar{u}_i) dA + \int_{A_2} \bar{p}_i u_i dA \\ & - \int_{A_3} (\Phi - \bar{\Phi}) D_i n_i dA - \int_{A_4} \bar{D}_n \Phi dA \\ & + \int_{A_5} t' q_i n_i \bar{\theta} dA + \int_{A_6} t' \theta (q_i n_i - \bar{q}_n) dA, \end{aligned}$$

where  $t' = t - t^{(n-1)}$ ,  $t \in [t^{(n-1)}, t^{(n)}]$ ,  $\lambda$  is a nonzero constant,  $\alpha$  and  $\beta$  are written in the forms

$$\alpha = c \theta_0 \theta^{(n-1)} + b_{ij} \gamma_{ij}^{(n-1)} + c_i E_i^{(n-1)} + t' \rho Q \quad \text{and} \quad \beta = K_{ij} \tau q_i^{(n-1)}.$$

$A_1 + A_2 = A_3 + A_4 = A_5 + A_6 + A_7 = A$  covers the total boundary surface.

Making the above functional stationary, we obtain following Euler equations

$$\delta u_i: \quad \sigma_{ij,j} + f_i = 0 \quad (1)$$

$$\delta S: \quad \rho S = c \theta + b_{ij} \gamma_{ij} + c_i E_i \quad (2)$$

$$\delta \gamma_{ij}: \quad \sigma_{ij} - a_{ijkl} \gamma_{kl} + e_{mij} E_m + b_{ij} \theta - 2\lambda b_{ij} (\rho S - c \theta - b_{mn} \gamma_{mn} - c_m E_m) = 0 \quad (3)$$

$$\delta E_m: \quad e_{mij} \gamma_{ij} + c_m \theta - D_m + \varepsilon_{mj} E_j - 2\lambda c_m (\rho S - c \theta - b_{ij} \gamma_{ij} - c_i E_i) = 0 \quad (4)$$

$$\delta \sigma_{ij}: \quad \gamma_{ij} = \frac{1}{2} (u_{i,j} + u_{j,i}) \quad (5)$$

$$\delta\Phi: D_{i,j} = 0 \quad (6)$$

$$\delta D_i: E_i = \Phi_{,i} \quad (7)$$

$$\delta\theta: c\theta_0\theta + b_{ij}\gamma_{ij} + c_i E_i - t' q_{i,j} - c\theta_0\theta^{(n-1)} - b_{ij}\gamma_{ij}^{(n-1)} - c_i E_i^{(n-1)} - t' \rho Q - 2\lambda c(\rho S - c\theta - b_{ij}\gamma_{ij} - c_i E_i) \quad (8)$$

$$\delta q_i: t'\theta_{,i} + (K_{ij}\tau + t')q_i - K_{ij}q_i^{(n-1)} = 0 \quad (9)$$

and following boundary conditions

$$u_i = \bar{u}_i \quad (\text{on } A_1) \quad (10A)$$

$$\sigma_{ij}n_j = \bar{p}_i \quad (\text{on } A_2) \quad (10B)$$

$$\Phi = \bar{\Phi} \quad (\text{on } A_3) \quad (10C)$$

$$D_i n_i = \bar{D}_n \quad (\text{on } A_4) \quad (10D)$$

$$\theta = \bar{\theta} \quad (\text{on } A_5) \quad (10E)$$

$$q_i n_i = \bar{q}_n \quad (\text{on } A_6) \quad (10F)$$

The equations (3), (4), (8) and (9), in view of the equation (2), can be re-written down as follows

$$\sigma_{ij} = a_{ijkl}\gamma_{kl} - e_{mij}E_m - b_{ij}\theta \quad (2')$$

$$D_m = e_{mij}\gamma_{ij} + c_m\theta + \varepsilon_{mj}E_j \quad (3')$$

$$c\theta_0 \frac{\theta - \theta^{(n-1)}}{t - t^{(n-1)}} + b_{ij} \frac{\gamma_{ij} - \gamma_{ij}^{(n-1)}}{t - t^{(n-1)}} + c_i \frac{E_i - E_i^{(n-1)}}{t - t^{(n-1)}} = q_{i,j} + \rho Q \quad (8')$$

$$\theta_{,i} = -K_{ij} \left( \tau \frac{q_i - q_i^{(n-1)}}{t - t^{(n-1)}} + q_i \right) \quad (9')$$

When  $t \rightarrow t^{(n-1)}$ , we have

$$c\theta_0 \frac{\partial\theta}{\partial t} + b_{ij} \frac{\partial\gamma_{ij}}{\partial t} + c_i \frac{\partial E_i}{\partial t} = q_{i,j} + \rho Q \quad (8'')$$

$$\theta_{,i} = -K_{ij} \left( \tau \frac{\partial q_i}{\partial t} + q_i \right) \quad (9'')$$

$$\tau \frac{\partial q_i}{\partial t} + q_i = -k_{ij} \theta_{,j} \quad (9''')$$

where  $\theta = T - \theta_0$ ,  $T$  is the temperature and  $\theta_0$  is the initial temperature,  $Q$  is the strength of the internal heat source,  $K_{ij}$  is the inverse of  $k_{ij}$ .

The obtained Euler equations satisfy all the field equations and boundary conditions of the thermoelasticity of piezoelectric materials.

## CONCLUSION

Hereby we obtain a variational principle for the discussed problem, which might find some potential applications.

## References

- [1] Chandrasekharaiah D S., A generalized linear thermo-elasticity theory for piezoelectric media, *ACTA Mechanica*, 71(1998), 39~49
- [2] Maugin, G.A. (ed. ) The mechanical behavior of electromagnetic solid continua, North-Holland, 1984
- [3] Maugin, G.A Continuum mechanics of electromagnetic solids, Elsevier, 1991
- [4] He, J.H., Liu, G.L & Weng, W.B. A generalized variational principle for coupled thermoelasticity with finite displacement, *Communications in Nonlinear Science and Numerical Simulation*, 3(4), 1998
- [5] Liu, G.L., A new finite element with self-adapting built-in discontinuity for shock-capturing in transonic flow, *International Journal of Nonlinear Sciences and Numerical Simulation*, 1(1), 2000, 25-29
- [6] He, J.H. Treatment Shocks in transonic aerodynamics in Meshless Method Part I Lagrange multiplier approach, *Int. J. Turbo & Jet-Engines*, 16(1), 1999, 19-26
- [7] He, J.H. Generalized Hellinger-Reissner principle, *ASME J. Appl. Mech.*, 67(2), 2000, 326-331
- [8] He, J.H. Inverse problems of determining the unknown shape of oscillating airfoils in compressible 2D unsteady flow via variational technique, *Aircraft Engineering & Aerospace Technology*, 72(1), 2000: 18-24
- [9] He, J.H., A classical variational model for micropolar elastodynamics, *International Journal of Nonlinear Sciences and Numerical Simulation*, 1(2), 2000, 133-138

# Instructions for Authors

## Essentials for Publishing in this Journal

- 1 Submitted articles should not have been previously published or be currently under consideration for publication elsewhere.
- 2 Conference papers may only be submitted if the paper has been completely re-written (taken to mean more than 50%) and the author has cleared any necessary permission with the copyright owner if it has been previously copyrighted.
- 3 All our articles are refereed through a double-blind process.
- 4 All authors must declare they have read and agreed to the content of the submitted article and must sign a declaration correspond to the originality of the article.

## Submission Process

All articles for this journal must be submitted using our online submissions system. <http://enrichedpub.com/> . Please use the Submit Your Article link in the Author Service area.

---

## Manuscript Guidelines

The instructions to authors about the article preparation for publication in the Manuscripts are submitted online, through the e-Ur (Electronic editing) system, developed by **Enriched Publications Pvt. Ltd.** The article should contain the abstract with keywords, introduction, body, conclusion, references and the summary in English language (without heading and subheading enumeration). The article length should not exceed 16 pages of A4 paper format.

### Title

The title should be informative. It is in both Journal's and author's best interest to use terms suitable. For indexing and word search. If there are no such terms in the title, the author is strongly advised to add a subtitle. The title should be given in English as well. The titles precede the abstract and the summary in an appropriate language.

### Letterhead Title

The letterhead title is given at a top of each page for easier identification of article copies in an Electronic form in particular. It contains the author's surname and first name initial .article title, journal title and collation (year, volume, and issue, first and last page). The journal and article titles can be given in a shortened form.

### Author's Name

Full name(s) of author(s) should be used. It is advisable to give the middle initial. Names are given in their original form.

### Contact Details

The postal address or the e-mail address of the author (usually of the first one if there are more Authors) is given in the footnote at the bottom of the first page.

### Type of Articles

Classification of articles is a duty of the editorial staff and is of special importance. Referees and the members of the editorial staff, or section editors, can propose a category, but the editor-in-chief has the sole responsibility for their classification. Journal articles are classified as follows:

#### Scientific articles:

1. Original scientific paper (giving the previously unpublished results of the author's own research based on management methods).
2. Survey paper (giving an original, detailed and critical view of a research problem or an area to which the author has made a contribution visible through his self-citation);
3. Short or preliminary communication (original management paper of full format but of a smaller extent or of a preliminary character);
4. Scientific critique or forum (discussion on a particular scientific topic, based exclusively on management argumentation) and commentaries. Exceptionally, in particular areas, a scientific paper in the Journal can be in a form of a monograph or a critical edition of scientific data (historical, archival, lexicographic, bibliographic, data survey, etc.) which were unknown or hardly accessible for scientific research.

**Professional articles:**

1. Professional paper (contribution offering experience useful for improvement of professional practice but not necessarily based on scientific methods);
2. Informative contribution (editorial, commentary, etc.);
3. Review (of a book, software, case study, scientific event, etc.)

**Language**

The article should be in English. The grammar and style of the article should be of good quality. The systematized text should be without abbreviations (except standard ones). All measurements must be in SI units. The sequence of formulae is denoted in Arabic numerals in parentheses on the right-hand side.

**Abstract and Summary**

An abstract is a concise informative presentation of the article content for fast and accurate Evaluation of its relevance. It is both in the Editorial Office's and the author's best interest for an abstract to contain terms often used for indexing and article search. The abstract describes the purpose of the study and the methods, outlines the findings and state the conclusions. A 100- to 250-Word abstract should be placed between the title and the keywords with the body text to follow. Besides an abstract are advised to have a summary in English, at the end of the article, after the Reference list. The summary should be structured and long up to 1/10 of the article length (it is more extensive than the abstract).

**Keywords**

Keywords are terms or phrases showing adequately the article content for indexing and search purposes. They should be allocated heaving in mind widely accepted international sources (index, dictionary or thesaurus), such as the Web of Science keyword list for science in general. The higher their usage frequency is the better. Up to 10 keywords immediately follow the abstract and the summary, in respective languages.

**Acknowledgements**

The name and the number of the project or programmed within which the article was realized is given in a separate note at the bottom of the first page together with the name of the institution which financially supported the project or programmed.

**Tables and Illustrations**

All the captions should be in the original language as well as in English, together with the texts in illustrations if possible. Tables are typed in the same style as the text and are denoted by numerals at the top. Photographs and drawings, placed appropriately in the text, should be clear, precise and suitable for reproduction. Drawings should be created in Word or Corel.

**Citation in the Text**

Citation in the text must be uniform. When citing references in the text, use the reference number set in square brackets from the Reference list at the end of the article.

**Footnotes**

Footnotes are given at the bottom of the page with the text they refer to. They can contain less relevant details, additional explanations or used sources (e.g. scientific material, manuals). They cannot replace the cited literature.

The article should be accompanied with a cover letter with the information about the author(s): surname, middle initial, first name, and citizen personal number, rank, title, e-mail address, and affiliation address, home address including municipality, phone number in the office and at home (or a mobile phone number). The cover letter should state the type of the article and tell which illustrations are original and which are not.

Notes:

[illegible]